Response to Anonymous Referee #1 – Development of iron-mediated molecular chlorine chemistry in GEOS-Chem: model description, evaluation and global atmospheric implication

We are grateful for the feedback and guidance of reviewer. The comments and concerns have been addressed carefully. Exact comments from the reviewer are in black italic type. Our responses (indent and in normal font) and the corresponding edits in the manuscript (indent and in blue) are shown below.

Comments from Anonymous Referee #1:

Chen et al. incorporate an iron-mediated molecular chlorine (Cl_2) formation mechanism into the GEOS-Chem model. They represent the dynamic solubility of iron (Fe) as a function of aerosol acidity, organic complexation, and mineralogical variability. The comparisons indicate that this newly implemented mechanism significantly improves the model's performance in simulating Cl_2 concentrations and substantially alters the global distribution of atmospheric oxidative capacity and subsequent fine particulate matter loadings. The manuscript is well-structured, the methodology is explicitly described, and the model evaluation is logically sound. The scope of this investigation is suitable for Atmospheric Chemistry and Physics. I recommend publication after the authors address the following questions.

Response in general: We thank the reviewer for the supportive and constructive suggestions.

Major question:

1. Lines 127-128: Please elaborate on the physical justification for mapping dust and non-dust Fe to the properties of fine-mode dust and hydrophilic/hydrophobic black carbon, respectively.

Response 1: Thanks for this comment. We assigned dust and non-dust Fe to different host templates by incorporating established methodologies from previous literature and considering their distinct emission sources and atmospheric transport characteristics.

Since the Fe(III)-mediated chlorine chemistry is primarily constrained to fine particles (Chen et al., 2024), herein we focus on the fine-mode tracers associated with the IMC mechanism. For dust Fe, the fine-mode dust Fe tracers follow the physical properties of the DST1 template (with a diameter < 2μm), including density and dry/wet deposition parameters. This is because dust-derived Fe is physically associated with mineral dust particles, and its atmospheric transport and removal should therefore be consistent with the corresponding fine-dust aerosol host. For non-dust Fe, the properties settings follow the methodology of Hamilton et al. (2019), in which fine-mode Fe from fires and anthropogenic combustion is assumed to have BC-like physical properties. This assumption is reasonable since non-dust Fe is mainly associated with combustion sources and is commonly co-emitted or mixed with carbonaceous aerosols such as BC during atmospheric transport. Accordingly, we assign non-dust Fe (including soluble and insoluble Fe) the physical properties of the corresponding BC (including hydrophilic and hydrophobic BC) species in GEOS-Chem. This treatment ensures that the simulated

Fe tracers undergo more physically reasonable atmospheric transport and scavenging processes. We have added the relevant details in the revised manuscript, as below.

Page 4 Line 129-130 in the revised manuscript: "Since the Fe(III)-mediated chlorine chemistry is primarily constrained to fine particles (Chen et al., 2024), eight new iron-bearing tracers associated with the IMC mechanism are introduced into the model."

Page 4 Line 139-144 in the revised manuscript: "In addition, each Fe tracer is assigned specific physical proxy properties to represent its atmospheric behaviors. Specifically, fine dust Fe follows the physical characteristics of fine-mode dust (DST1), including its prescribed density and deposition parameters. For non-dust Fe, we adopt the physical characteristics of black carbon, as these iron species are typically co-emitted and internally mixed with carbonaceous aerosols. Soluble and insoluble non-dust Fe is further mapped to hydrophilic and hydrophobic host species, respectively. This treatment ensures that the simulated Fe tracers undergo more physically reasonable atmospheric transport and scavenging processes."

2. Line 165: In Equation 4, the formulation relies on the term Max[SOA]. Please explicitly define this term. Does it represent a global spatial maximum or a temporal maximum at a specific grid box?

Response 2: Thanks for this comment. Max[SOA] represents the global maximum SOA concentration diagnosed from the model SOA field, rather than a temporal maximum at a specific grid box. It is used as a fixed normalization constant to scale the SOA-dependent oxalate proxy in Eq.(4) following Hamilton et al. (2019) and Scanza et al. (2018). We have clarified this definition in the revised manuscript, as below.

Page 5 Line 185-186 in the revised manuscript: "Max[SOA] denotes the global maximum SOA concentration diagnosed from the standard simulation."

3. Figure 1(a): The global distribution shows uncharacteristically high Fe concentrations compared to observations over southern South America. What is the primary emission source driving these high values in the model? If this is attributed to biomass burning, the low solubility shown in Figure 1(b) contradicts the characteristically high initial solubility of biomass-burning Fe.

Response 3: To identify the source responsible for the relatively high Fe concentrations over southern South America, we performed a source-resolved Fe attribution simulation. As shown in Fig. R1, the enhanced Fe concentrations in this region are dominated by dust-derived Fe, rather than biomass-burning Fe.

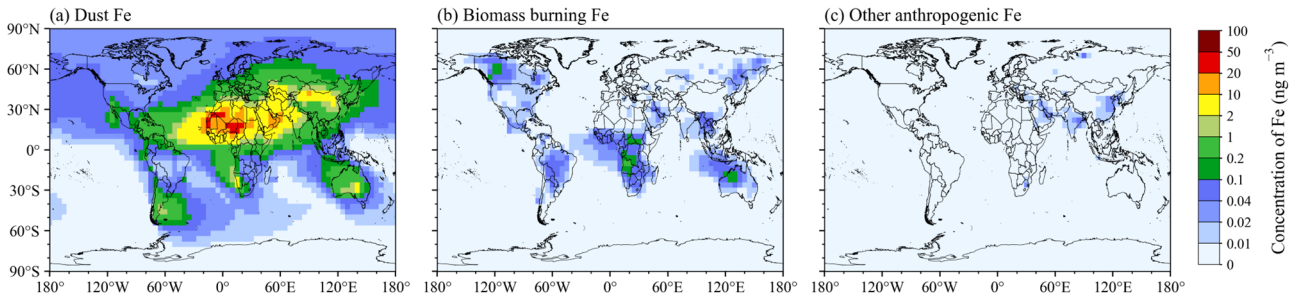

Figure R1. Spatial distributions of annual mean aerosol Fe concentrations contributed by (a) dust, (b) biomass burning, and (c) other anthropogenic sources.

In particular, this region is located close to Patagonia desert, which has been identified as one of the major dust source regions in the Southern Hemisphere (Gassó and Stein, 2007; Johnson et al., 2010; Paparazzo et al., 2018; Demasy et al., 2024). Recent source-attribution results from the AeroCom-III/DUSA multi-model experiments also indicate that Patagonia is an important contributor to southern hemisphere atmospheric dust loading (Kim et al., 2024). Therefore, the high Fe concentrations simulated over southern South America are more consistent with strong contributions from Patagonian dust emissions. Fe in this region is mainly associated with mineral dust which largely present in relatively insoluble mineral forms such as hematite, illite, and smectite. In addition, the region is close to the dust source, where atmospheric aging processes that enhance Fe solubility, including acid processing and organic complexation, are relatively limited. As a result, Fe exhibits a generally low solubility in this area. We have added Fig. R1 to the revised supplementary material (as Fig. S3) and incorporated relevant discussions into the revised manuscript, as below.

Page 7 Line 258-261 in the revised manuscript: "A localized enhancement is also simulated over southern South America, mainly reflecting the contribution of dust-derived Fe from the Patagonian dust source region (Fig. S3), which has been identified as an important dust source in the Southern Hemisphere (Demasy et al., 2024; Gassó and Stein, 2007; Paparazzo et al., 2018)."

Page 8 Line 273-275 in the revised manuscript: "A similar feature is found over southern South America, where the enhanced Fe is mainly associated with freshly emitted Patagonian dust. The low solubility in this region is therefore consistent with the dominance of relatively insoluble mineral Fe phases and the limited atmospheric aging near the dust source."

4. Figure 1(b): How do the authors explain the high modeled Fe solubility in the mid-to-high latitudes of North America compared to the lower solubility in East Asia? Given that both regions experience frequent open biomass burning, which should emit highly soluble Fe, this regional discrepancy requires further clarification.

Response 4: Thanks for this comment. As shown by the Fe source-apportionment results presented in Response 3 (Fig. R1), the regional contrast in Fe solubility is closely related to differences in the dominant Fe

sources. The relatively high Fe solubility over the mid-to-high latitudes of North America is associated with the stronger contribution of biomass-burning Fe, particularly over boreal fire-influenced regions. Since biomass burning generally emits Fe with higher initial solubility, its larger relative contribution increases the bulk aerosol Fe solubility in this region. In contrast, although open biomass burning also occurs in East Asia, biomass-burning Fe contributes only a minor fraction of the annual mean aerosol Fe burden there. The total Fe concentration over East Asia is instead strongly influenced by mineral dust and other anthropogenic Fe sources, which generally correspond to the low-initial-solubility Fe categories in our model. Previous studies have shown that natural dust from the Taklimakan and Gobi deserts can be transported eastward and southward, supplying dust-derived Fe to East Asia and the Northwest Pacific (Zhu et al., 2025). In addition, anthropogenic fugitive, combustion, and industrial dust emissions are particularly important over East and South Asia (Philip et al., 2017). Consistently, source-apportionment analysis of East Asian outflow aerosols shows that fine-particle Fe is mainly associated with fresh/aged dust and anthropogenic sources such as the steel industry, with dominant Fe-bearing phases including aluminosilicates and Fe-oxide nanoparticles (Bunnell et al., 2025; Sakata et al., 2025). As a result, the soluble Fe signal from biomass burning is diluted by these lower-solubility sources, leading to lower modelled bulk Fe solubility over East Asia than over the mid-to-high latitudes of North America. We have added this clarification in the revised manuscript, as below.

Page 8 Line 277-285 in the revised manuscript: "In addition to atmospheric processing, regional differences in Fe source composition also contribute to the spatial variability of Fe solubility. Although both mid-to-high-latitude North America and East Asia experience frequent open biomass burning, they exhibit distinct Fe solubility patterns. As shown in Fig. S3, the relatively high solubility over northern North America is mainly associated with the stronger contribution of boreal biomass-burning Fe, which is represented with relatively high initial solubility in the model. In East Asia, however, aerosol Fe is mainly from mineral dust transported from the Taklimakan and Gobi deserts, as well as anthropogenic fugitive, combustion, and industrial Fe sources (Philip et al., 2017; Zhu et al., 2025; Bunnell et al., 2025; Sakata et al., 2025), which generally correspond to lower Fe solubility. Therefore, the biomass-burning Fe signal is largely diluted by these larger Fe inputs, leading to lower bulk Fe solubility over East Asia despite the occurrence of biomass burning."

5. Lines 357-359: In NOx-rich regions, the enhanced OH and HO_2 are also contributed by the nighttime $ClNO_2$ chemistry.

Response 5: Thanks for this helpful comment. We have added a discussion in the revised manuscript to acknowledge the contribution of nighttime $ClNO_2$ chemistry to enhanced OH and HO_2 in NO*x*-rich regions, as below.

Page 12 Line 410-412 in the revised manuscript: "This enhancement is also partly contributed by nighttime $ClNO_2$ chemistry, as nocturnal $ClNO_2$ formation followed by morning photolysis provides an additional Cl

radical source, further promoting HO_2 production and subsequent OH regeneration (Liu et al., 2017; Riedel et al., 2014).

6. Lines 390-393: The authors attribute the increase in nitrate in the North China Plain to Cl-initiated OH enhancements. However, Figure S5 shows a concurrent decrease in sulfate in this region. Since elevated OH should accelerate SO_2 oxidation and increase sulfate, please further discuss the contraction.

Response 6: Thanks for this comment. Previous studies have shown that daytime nitrate formation is primarily controlled by the OH-initiated NO_2 oxidation and subsequent gas–particle partitioning (Liu et al., 2020; Wang et al., 2026), the strengthened oxidizing environment accelerates nitrate formation and thereby increases $PM_{2.5}$ mass concentration (Feng et al., 2021; Fu et al., 2020; Zang et al., 2022). In this study, the increase in Cl_2 over the NCP generates Cl radicals through photolysis, which further elevates regional OH levels and accelerates the conversion of NO*x* to nitrate.

In contrast, sulfate formation is jointly influenced by multiple SO_2 oxidation pathways, including gas-phase reactions with OH radicals or stabilized Criegee intermediates, heterogeneous-phase reactions on the surface of particles, and aqueous-phase reactions with dissolved O_3, NO_2, H_2O_2, and organic peroxides, as well as autoxidation catalyzed by transition metals (Liu et al., 2020; Guo et al., 2024; Gao et al., 2024; He et al., 2025). In addition to these conventional pathways, hydroxymethanesulfonate (HMS) formed through the reaction between dissolved SO_2 and HCHO can subsequently be oxidized by aqueous OH radicals to sulfate (Song et al., 2019, Ma et al., 2020, Dovrou et al., 2022). In this study, the enhanced iron-chlorine chemistry simultaneously elevates regional OH levels and promotes HCHO production which further increases the concentration of HMS (as shown in Fig. R2a). On the one hand, this process competitively consumes precursors (SO_2) that would otherwise be available for direct oxidation to sulfate. On the other hand, since HMS is relatively stable under acidic conditions and resistant to oxidation by common aqueous oxidants such as H_2O_2 or O_3 (Dovrou et al., 2022), sulfate production via HMS oxidation may not fully compensate for the suppression of conventional formation routes. Consequently, sulfate concentrations slightly decrease over the NCP despite the enhanced OH levels.

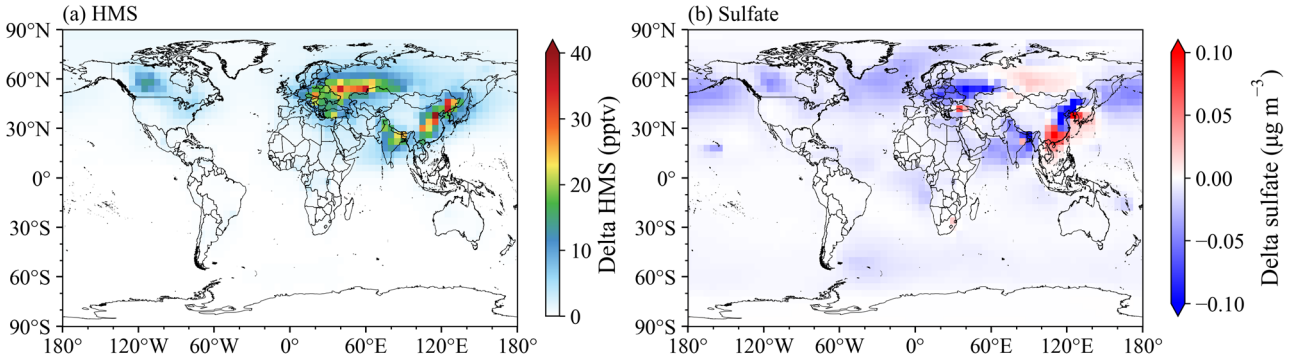

Figure R2. Absolute changes (VarFeS-Base) of annual mean surface concentration of (a) HMS and (b) sulfate.

We have enriched our discussion in the revised manuscript, as below.

Page 13 Line 475-484 in the revised manuscript: "Under conditions of enhanced HO*x* cycling, nitrate and sulfate do not respond uniformly to the IMC mechanism. While nitrate formation is primarily driven by increased OH oxidation (Liu et al., 2020; Wang et al., 2026), sulfate production is governed not only by gas-phase OH oxidation of SO_2 but also by aqueous, heterogeneous, and transition-metal-catalyzed oxidation pathways (Guo et al., 2024; Gao et al., 2024; He et al., 2025). Besides, hydroxymethanesulfonate (HMS) formed through the reaction between dissolved SO_2 and HCHO can subsequently be oxidized by aqueous OH radicals to sulfate (Song et al., 2019, Ma et al., 2020, Dovrou et al., 2022). Though elevated regional OH levels promote HCHO production which further increases the concentration of HMS (Fig.S12), HMS formation may temporarily sequester precursor SO_2, and its subsequent oxidation is likely insufficient to offset the suppression of sulfate formation via direct SO_2 oxidation. Therefore, sulfate concentrations slightly decrease over the NCP despite the enhanced OH levels."

Minor suggestions:

1. Please add a global distribution map for soluble Fe, which could better illustrate the impact of the iron-mediated Cl_2 formation mechanism on Cl_2.

Response 7: We have added a figure to display the global distribution map for soluble Fe in the revised supplementary material, as shown in below.

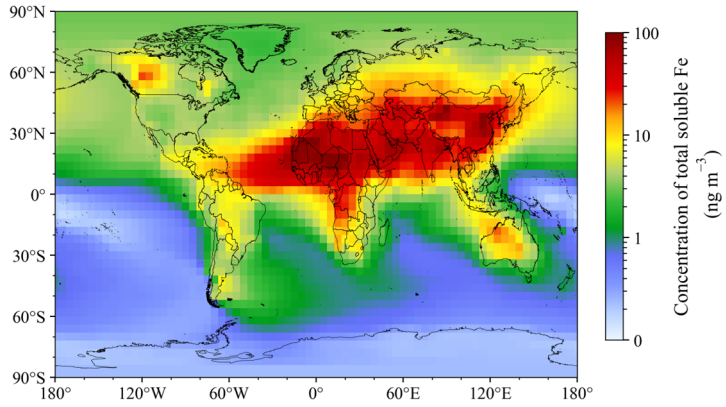

Figure R3. Global distributions of annual mean total soluble Fe concentrations.

We have also added the corresponding description in the revised manuscript, as below.

Page 10 Line 337-339 in the revised manuscript: "Wildfires simultaneously release large amounts of soluble Fe and pCl aerosols from biomass burning within a short period (Tang et al., 2021; Zhang et al., 2022) (the corresponding distribution of soluble Fe concentration is shown in Fig. S6), thereby eliminating precursor limitations on Cl_2 formation processes."

Page 10 Line 351-353 in the revised manuscript: “Although dust-bound Fe possesses lower solubility, the massive total flux ensures that soluble Fe concentrations (43.5 ± 19.0 ng m^{-3}) far above the global mean (7.1 ± 14.8 ng m^{-3}) (Fig. S6), coupled with abundant sea-salt chloride emissions, maintains a stable Cl_2 background in TA.”

References:

Bunnell, Z. B., Sieber, M., Hamilton, D. S., Marsay, C. M., Buck, C. S., Landing, W. M., John, S. G., and Conway, T. M.: The Influence of natural, anthropogenic, and wildfire sources on iron and zinc aerosols delivered to the north Pacific Ocean, Geophys. Res. Lett., 52,doi: 10.1029/2024gl113877, 2025.

Chen, Q., Wang, X., Fu, X., Li, X., Alexander, B., Peng, X., Wang, W., Xia, M., Tan, Y., Gao, J., Chen, J., Mu, Y., Liu, P., and Wang, T.: Impact of molecular chlorine production from aerosol iron photochemistry on atmospheric oxidative capacity in north China, Environ. Sci. Technol., 58, 12585-12597,doi: 10.1021/acs.est.4c02534, 2024.

Demasy, C., Boye, M., Lai, B., Burckel, P., Feng, Y., Losno, R., Borensztajn, S., and Besson, P.: Iron dissolution from Patagonian dust in the Southern Ocean: under present and future conditions, Front. Mar. Sci., 11,doi: 10.3389/fmars.2024.1363088, 2024.

Dovrou, E., Bates, K. H., Moch, J. M., Mickley, L. J., Jacob, D. J., and Keutsch, F. N.: Catalytic role of formaldehyde in particulate matter formation, Proc Natl Acad Sci U S A, 119,doi: 10.1073/pnas.2113265119, 2022.

Feng, T., Bei, N., Zhao, S., Wu, J., Liu, S., Li, X., Liu, L., Wang, R., Zhang, X., Tie, X., and Li, G.: Nitrate debuts as a dominant contributor to particulate pollution in Beijing: Roles of enhanced atmospheric oxidizing capacity and decreased sulfur dioxide emission, Atmos. Environ., 244,doi: 10.1016/j.atmosenv.2020.117995, 2021.

Fu, X., Wang, T., Gao, J., Wang, P., Liu, Y. M., Wang, S. X., Zhao, B., and Xue, L. K.: Persistent heavy winter nitrate pollution driven by increased photochemical oxidants in northern China, Environ. Sci. Technol., 54, 3881-3889,doi: 10.1021/acs.est.9b07248, 2020.

Gassó, S. and Stein, A. F.: Does dust from Patagonia reach the sub-Antarctic Atlantic ocean?, Geophys. Res. Lett., 34,doi: 10.1029/2006gl027693, 2007.

Gao, J., Wang, H., Liu, W., Xu, H., Wei, Y., Tian, X., Feng, Y., Song, S., and Shi, G.: Hydrogen peroxide serves as pivotal fountainhead for aerosol aqueous sulfate formation from a global perspective, Nat. Commun., 15, 4625,doi: 10.1038/s41467-024-48793-1, 2024.

Guo, Z. Y., Lu, K. D., Qiu, P. X., Xu, M. Y., and Guo, Z. B.: Quantifying SO_2 oxidation pathways to atmospheric sulfate using stable sulfur and oxygen isotopes: laboratory simulation and field observation, Atmos. Chem. Phys., 24, 2195-2205,doi: 10.5194/acp-24-2195-2024, 2024.

Hamilton, D., Scanza, R., Yan, F., Guinness, J., Kok, J., Li, L., Liu, X., Rathod, S., Wan, J. S., Wu, M., and Mahowald, N.: Improved methodologies for Earth system modelling of atmospheric soluble iron and observation comparisons using the Mechanism of Intermediate complexity for Modelling Iron (MIMI v1.0), Geosci. Model Dev., 12, 3835-3862,doi: 10.5194/GMD-12-3835-2019, 2019.

He, P. Z., Chi, X. Y., Zhang, B. H., Hua, C., Dao, X., Meng, X. Y., and Ma, T. M.: Exploring the formation of atmospheric nitrate and sulfate based on one-year observations in Beijing, Aerosol Sci. Eng.,doi: 10.1007/s41810-025-00361-w, 2025.

Johnson, M. S., Meskhidze, N., Solmon, F., Gassó, S., Chuang, P. Y., Gaiero, D. M., Yantosca, R. M., Wu, S. L., Wang, Y. X., and Carouge, C.: Modeling dust and soluble iron deposition to the South Atlantic Ocean, J Geophys Res-Atmos, 115,doi: 10.1029/2009jd013311, 2010.

Kim, D., Chin, M., Schuster, G., Yu, H. B., Takemura, T., Tuccella, P., Ginoux, P., Liu, X. H., Shi, Y., Matsui, H., Tsigaridis, K., Bauer, S. E., Kok, J. F., and Schulz, M.: Where dust comes from: Global assessment of dust source aattributions with AeroCom Models, J Geophys Res-Atmos, 129,doi: 10.1029/2024jd041377, 2024.

Liu, P. F., Ye, C., Xue, C. Y., Zhang, C. L., Mu, Y. J., and Sun, X.: Formation mechanisms of atmospheric nitrate and sulfate during the winter haze pollution periods in Beijing: gas-phase, heterogeneous and aqueous-phase chemistry, Atmos. Chem. Phys., 20, 4153-4165,doi: 10.5194/acp-20-4153-2020, 2020.

Ma, T., Furutani, H., Duan, F., Kimoto, T., Jiang, J., Zhang, Q., Xu, X., Wang, Y., Gao, J., Geng, G., Li, M., Song, S., Ma, Y., Che, F., Wang, J., Zhu, L., Huang, T., Toyoda, M., and He, K.: Contribution of hydroxymethanesulfonate (HMS) to severe winter haze in the North China Plain, Atmos. Chem. Phys., 20, 5887-5897,doi: 10.5194/acp-20-5887-2020, 2020.

Paparazzo, F., Crespi-Abril, A., Gonçalves, R., Barbieri, E., Gracia Villalobos, L., Solís, M., and Soria, G.: Patagonian dust as a source of macronutrients in the Southwest Atlantic Ocean, Oceanography, 31, 33-39,doi: 10.5670/oceanog.2018.408, 2018.

Philip, S., Martin, R. V., Snider, G., Weagle, C. L., van Donkelaar, A., Brauer, M., Henze, D. K., Klimont, Z., Venkataraman, C., Guttikunda, S. K., and Zhang, Q.: Anthropogenic fugitive, combustion and industrial dust is a significant, underrepresented fine particulate matter source in global atmospheric models, Environ. Res. Lett., 12, 044018,doi: 10.1088/1748-9326/aa65a4, 2017.

Sakata, K., Takano, S., Matsuki, A., Takeichi, Y., Tanimoto, H., Sakaguchi, A., Kurisu, M., and Takahashi, Y.: Atmospheric chemistry in East Asia determines the iron solubility of aerosol particles supplied to the North Pacific Ocean, Atmos. Chem. Phys., 25, 11087-11107,doi: 10.5194/acp-25-11087-2025, 2025.

Song, S., Gao, M., Xu, W., Sun, Y., Worsnop, D. R., Jayne, J. T., Zhang, Y., Zhu, L., Li, M., Zhou, Z., Cheng, C., Lv, Y., Wang, Y., Peng, W., Xu, X., Lin, N., Wang, Y., Wang, S., Munger, J. W., Jacob, D. J., and McElroy, M. B.: Possible heterogeneous chemistry of hydroxymethanesulfonate (HMS) in northern China winter haze, Atmos. Chem. Phys., 19, 1357-1371,doi: 10.5194/acp-19-1357-2019, 2019.

Scanza, R., Hamilton, D., García-Pando, C. P., Buck, C., Baker, A., and Mahowald, N.: Atmospheric processing of iron in mineral and combustion aerosols: development of an intermediate-complexity mechanism suitable for Earth system models, Atmos. Chem. Phys., 18, 14175-14196,doi: 10.5194/ACP-18-14175-2018, 2018.

Wang, J. Q., Du, X. H., Wen, L., Che, F., Zhang, Y. C., and Gao, J.: Particulate nitrate pollution control in North China Plain and Northeastern United States: A comparison of formation mechanism and its response to gaseous pollutants, Environ. Pollut., 397,doi: 10.1016/j.envpol.2026.127939, 2026.

Zang, H., Zhao, Y., Huo, J. T., Zhao, Q. B., Fu, Q. Y., Duan, Y. S., Shao, J. Y., Huang, C., An, J. Y., Xue, L. K., Li, Z. Y., Li, C. X., and Xiao, H. Y.: High atmospheric oxidation capacity drives wintertime nitrate pollution in the eastern Yangtze River Delta of China, Atmos. Chem. Phys., 22, 4355-4374,doi: 10.5194/acp-22-4355-2022, 2022.

Zhu, H. Z., Liu, Y. M., Yue, M., Feng, S. H., Fu, P. Q., Huang, K., Dong, X. Y., and Wang, M. H.: Trends and drivers of soluble iron deposition from East Asian dust to the Northwest Pacific: a springtime analysis (2001-2017), Atmos. Chem. Phys., 25, 5175-5197,doi: 10.5194/acp-25-5175-2025, 2025.